View metadata, citation and similar papers at core.ac.uk
brought to you by CORE
provided by RERO DOC Digital Library

Biomimetic mechanically adaptive nanocomposites

Kadhiravan Shanmuganathan [a], Jeffrey R. Capadona [a,b,d], Stuart J. Rowan [a,b,c,**], Christoph Weder [a,c,e,*]

[a] Department of Macromolecular Science and Engineering, Case Western Reserve University, 2100 Adelbert Road, Cleveland, OH 44106, USA
[b] Department of Biomedical Engineering, Case Western Reserve University, 10900 Euclid Avenue, Cleveland, OH 44106, USA
[c] Department of Chemistry, Case Western Reserve University, 2100 Adelbert Road, Cleveland, OH 44106, USA
[d] Rehabilitation Research and Development, Louis Stokes Cleveland DVA Medical Center, 10701 East Blvd., Cleveland, OH 44106, USA
[e] Adolphe Merkle Institute, University of Fribourg, Route de l'ancienne Papeterie CP 209, CH 1723 Marly 1, Switzerland

The development of a new class of mechanically adaptive nanocomposites has been inspired by biological creatures such as sea cucumbers, which have the ability to reversibly change the stiffness of their dermis. Several recent studies have related this dynamic mechanical behaviour to the distinctive nanocomposite architecture of the collagenous tissue, in which interactions among rigid collagen fibrils, embedded in a viscoelastic matrix of fibrillin microfibrils, are regulated by neurosecretory proteins. Here we review the development of a new family of artificial polymer nanocomposites that mimic the architecture and the mechanic adaptability of the sea cucumber dermis. The new materials are based on low-modulus matrix polymers that are reinforced with a percolating cellulose nanofiber network. Owing to the abundance of surface hydroxyl groups, the cellulose nanofibers display strong interactions between themselves, causing the evenly dispersed percolating nanocomposites to display a high stiffness. The nanofiber–nanofiber interactions can be largely switched off by the introduction of a chemical regulator that allows for competitive hydrogen bonding, resulting in a significant decrease in the stiffness of the material.

http://doc.rero.ch

Contents

1. Introduction

Polymers which change their mechanical properties "on command", i.e. upon exposure to a pre-defined stimulus in a highly selective and reversible manner, are

* Corresponding author. Tel.: +41 26 300 9465; fax: +41 26 300 9624.
** Corresponding author. Tel.: +1 216 368 4242; fax: +1 216 368 4202.
E-mail addresses: stuart.rowan@case.edu (S.J. Rowan), christoph.weder@case.edu (C. Weder).

0079-6700/$ – see front matter © 2009 Elsevier Ltd. All rights reserved.
doi:10.1016/j.progpolymsci.2009.10.005

http://doc.rero.ch

attractive for countless technologically relevant applications [1]. Shape-memory polymers, which have the ability to return from a deformed state to their original shape through a temperature increase (or exposure to other stimuli that cause a temperature increase in the material) represent a design approach that is currently receiving much attention [2–5]. Other classes of widely investigated mechanically adaptable materials include temperature and chemo-responsive polymer (hydro)gels and networks [6–8], photo-responsive gels [9], liquid–crystalline elastomers [10], electro-rheological fluids and gels [11], as well as materials that undergo dimensional changes upon stimulation, for example electrostrictive materials [12]. While the mechanical changes of these materials can be quite dramatic – some exhibit viscosity/modulus changes of several orders of magnitude – the large majority of these mechano-responsive materials exhibit a very low modulus [13]. While their property profiles are ideal for applications such as drug delivery [14], cell culturing [15], or actuation [12], examples of much stiffer materials that exhibit such morphing mechanical behaviour are limited. In this paper we review some of our recent work directed toward the development of a new class of mechanically switchable materials, which was inspired by the mechanism responsible for the morphing mechanical properties displayed by the inner dermis of sea cucumbers.

2. The biological model

Many echinoderms (e.g. sea cucumbers, starfish, etc.) share the ability to rapidly and reversibly alter the stiffness of their connective tissue [16]. In the case of, for example, sea cucumbers (Fig. 1a), this morphing occurs within seconds and creates significant survival advantages [17]. A series of recent studies on the collageneous inner dermis of these invertebrates has provided strong evidence that this interesting defence mechanism is enabled by a nanocomposite structure that involves rigid, high-aspect ratio collagen fibrils that lack permanent associations and are organised within a viscoelastic matrix of fibrillin microfibrils (Fig. 1b) [18–20]. The stiffness of the tissue depends on the ability of adjacent collagen fibrils to transfer stress via transiently established interactions [21,22]. These interactions are regulated by soluble molecules that are secreted locally by neurally controlled effector cells. A constitutive glycoprotein of the extracellular matrix, stiparin, was reported to induce aggregation of isolated fibrils and initially identified as a tissue-stiffening factor [23]. A second glycoprotein, stiparin inhibitor, was shown to bind to stiparin, thereby inhibiting its ability to induce fibril aggregation [24]. More recently, a third component, tensilin, was discovered, which not only induces collagen-fibril aggregation in vitro, but also increases tissue stiffness and appears to play an important role [25,26]. However, a detailed molecular mechanism for the regulation of collagen-fibril associations in the sea cucumber dermis has yet to be developed. Nonetheless, the dermis of the *Cucumaria frondosa* (and other sea cucumber species) represents a compelling model of a chemo-responsive material in which a 10-fold modulus contrast (ca. 5–50 MPa) is possible [27]. Intrigued by this capability, we set out to investigate if artificial polymer nanocomposites (Fig. 1b) can be created that exhibit similar architecture and chemo-mechanical behaviour.

3. Theoretical models for nanocomposite mechanics

The mechanical morphing of nanocomposites as a result of changing nanoparticle interactions can be described in the framework of two limiting mechanical models that are commonly used to describe the stiffness of nanocomposites with high-aspect ratio nanofillers: percolation and mean-

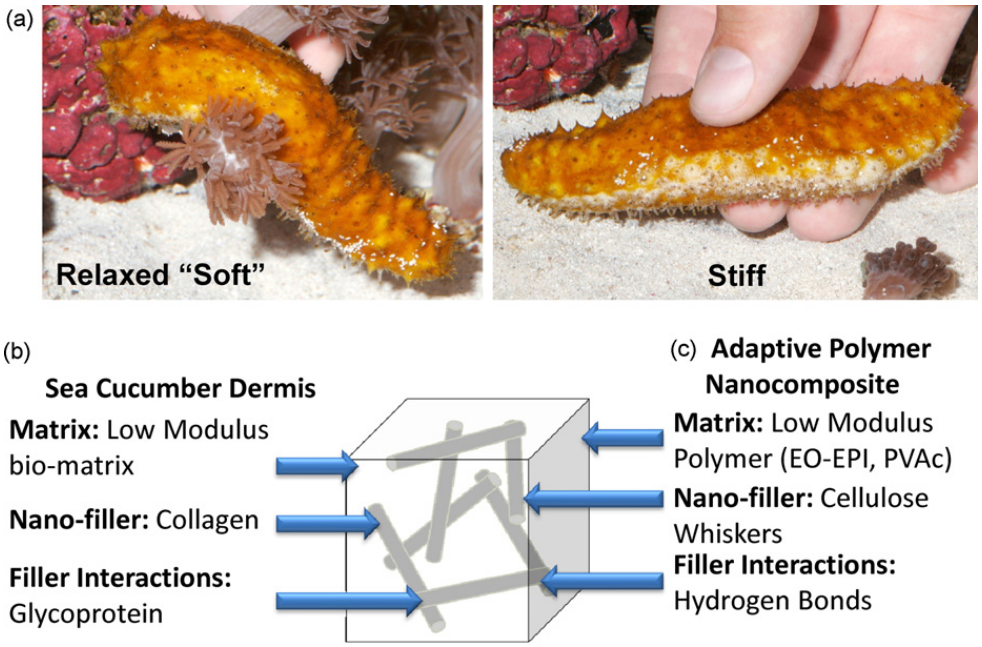

Fig. 1. (a) Picture of the natural model, a sea cucumber, in the relaxed soft state and the stiffened state (Reprinted from Ref. [58]), (b) the proposed biological nanocomposite model found in the sea cucumber dermis and (c) the proposed retro-engineered biomimetic nanocomposite material.

field models. These theoretical approaches are employed to predict the expected tensile storage modulus of the nanocomposite, E'_c (which can be converted into the shear modulus of the composite, assuming that the whisker sheets are mechanically isotropic $G' = E'/(2(1+\nu))$, $\nu = 0.3$ for rigid systems [28]) taking into account the experimentally determined mechanical properties of the pure soft (polymer matrix) and rigid (nanofiber) components (tensile storage moduli, E'_s and E'_r, respectively), the volume fraction of the rigid nanofiber, X_r, as well as their dimensions (expressed by the aspect ratio, A).

Within the scope of the percolation model (Eq. (1)), which was originally used by Takayanagi et al. [29] for semicrystalline polymers and Ouali et al. [30] for phase-separated blends and subsequently applied by Cavaillé for polymer/cellulose nanofiber composites [31], the high-aspect ratio filler particles are assumed to interact with each other to form a percolating network; the modulus of the composite (above T_g) is assumed to primarily depend on this percolating network of rigid rod-like fillers. Within this model, E'_c is expressed by:

$$E'_c = \frac{(1-2\psi+\psi X_r)E'_s E'_r + (1-X_r)\psi E'^2_r}{(1-X_r)E'_r + (X_r-\psi)E'_s} \quad (1)$$

where ψ is the percolating volume fraction of whiskers that participate in the load transfer, which using percolation theory can be estimated with Eq. (2):

$$\psi = X_r\left(\frac{X_r - X_c}{1-X_c}\right)^{0.4} \quad (2)$$

assuming that $X_r \geq X_c$, where X_c, which equals $0.7/A$ [32], is the critical filler volume fraction needed for percolation (percolation threshold).

By contrast, a mean-field approach is the basis for the Halpin–Kardos model [33], which expresses E'_c by:

$$E'_c = \frac{4U_5(U_1 - U_5)}{U_1} \quad (3)$$

with

$$U_1 = 1/8(3Q_{11} + 3Q_{22} + 2Q_{12} + 4Q_{66})$$

$$U_5 = 1/8(Q_{11} + Q_{22} - 2Q_{12} + 4Q_{66})$$

$$Q_{11} = \frac{E'_L}{(1-\nu_{12}\nu_{21})}$$

$$Q_{22} = E'_T(1-\nu_{12}\nu_{21})$$

$$Q_{12} = \nu_{12}Q_{22} = \nu_{21}Q_{11}$$

$$Q_{66} = G'_{12};$$

where $\nu_{12} = \phi_r\nu_r + \phi_s\nu_s$; $G'_{12} = G'_s(1+\eta\phi_r)/(1-\eta\phi_r)$; $\eta = (G'_r/G'_s - 1)/(G'_r/G'_s + 1)$ and ν is the Poisson's ratio (defined above as 0.3), G' is the shear modulus and ϕ is equal to the volume fraction of the phase (subscripts r and s refer to the rigid filler and soft polymer phases, respectively).

The model assumes that the materials are "quasi-isotropic" and are constituted by many layers of unidirectional plies oriented in alternating directions ($-45°$, $0°$, $45°$, and $90°$). The properties of the unidirectional reference ply are predicted by the Halpin–Tsaï equations (Eq. (4)) where the modulus in the longitudinal (E'_L) and transverse (E'_T) directs are given by [34,35]:

$$E'_L = \frac{E'_s(1+2(A)\eta_L\phi_r)}{(1-\eta_L\phi_r)} \text{ and } E'_T = \frac{E'_s(1+2\eta_T\phi_r)}{(1-\eta_T\phi_r)} \quad (4)$$

where $\eta_L = ((E_{lr}/E_s)-1)/((E_{lr}/E_s)+2A)$, and $\eta_T = ((E_{tr}/E_s)-1)/((E_{tr}/E_s)+2)$.

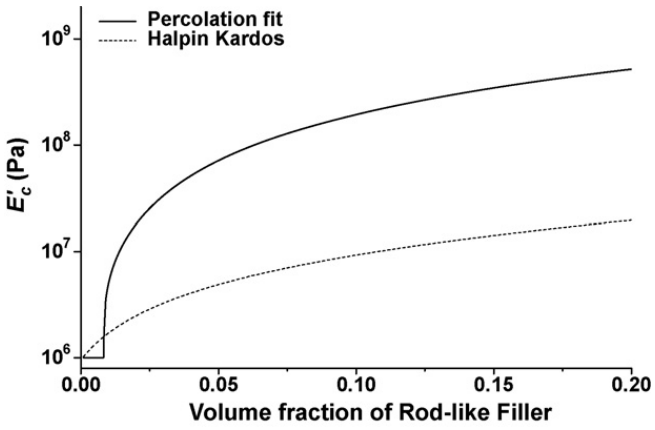

Fig. 2. Calculated tensile storage moduli E'_c of nanocomposites composed of a soft polymer matrix and a rigid rod-like nanofiller as a function of filler volume fraction. E'_c was calculated using the percolation (Eqs. (1) and (2)) and Halpin–Kardos (Eqs. (3) and (4)) models, which describe the limiting cases in which the filler–filler interactions are switched "on" or "off", respectively. The following assumptions were made: Tensile modulus of the neat matrix polymer $E'_s = 1$ MPa (in both on and off state), tensile modulus of the neat filler $E'_r = 5$ GPa, Poisson's ratio of both polymer and filler ν_s and $\nu_r = 0.3$, aspect ratio of the filler $A = 100$, longitudinal filler modulus $E'_{lf} = 130$ GPa, transverse filler modulus $E'_{tf} = 5$ GPa, filler shear modulus $E'_r = 1.77$ GPa [35,36].

This model has been successfully used to describe the modulus of nanocomposites in which the filler is homogeneously dispersed in a polymer matrix and does not display pronounced filler–filler interactions [34]. Thus, the percolation model would be appropriate to describe the mechanical properties of the natural and artificial nanocomposites according to Fig. 1 under the assumption that the fibre interactions are switched "on" [36], while the Halpin–Kardos model should accurately describe the moduli of these materials when the fibre interactions are switched "off". A comparison of the two models allows one to predict the expected changes of the nanocomposite's modulus, E'_c, upon switching the fibre interactions on the basis of experimentally determined quantities for the neat components. Fig. 2 shows sample calculations based on data that are realistic for the materials systems investigated by us (vide infra), which clearly indicate that large mechanical contrasts (more than an order of magnitude) can be achieved by this approach.

4. Synthetic dynamic nanocomposites

4.1. Cellulose whisker nanofiller

Retro-engineering of the biological model, i.e. the sea cucumber dermis (Fig. 1b), resulted in the blueprints of a synthetic nanocomposite (Fig. 1c) in which interactions

http://doc.rero.ch

between the rigid fillers can be switched on and off [37] in response to a chemical stimulus. A low-modulus synthetic polymer matrix replaces the viscoelastic matrix of fibrillin microfibrils found in the natural model. Instead of collagen fibrils we employed cellulose nanofibers as the rigid filler; their interactions are controlled by hydrogen bonding between surface hydroxyl groups. Within this framework, a chemical regulator that can disrupt this hydrogen bonding can be used to replace the (glyco)proteins used in the natural model. It should be noted that unlike in the biological model, where the soft state is the "relaxed" natural state, in this synthetic model the "unregulated" state is the stiff state.

Cellulose nanofibers (commonly referred to as "whiskers") can be isolated from a variety of renewable sources, including plants (such as wood, cotton, or wheat straw), as well as from bacterial sources or animal (e.g. tunicates) tissue. Such whiskers have been used to reinforce numerous polymer matrices, and the mechanisms of their reinforcement have been studied extensively through experiments and theoretical studies [38–41]. Owing to their strongly interacting surface hydroxyl groups, cellulose whiskers have a strong tendency for self-association [42]. This is, in principle, a very desirable feature for the formation of load-bearing percolating architectures within a polymer matrix. The significant reinforcement observed for polymer/cellulose whisker nanocomposites can be attributed to the formation of rigid whisker networks in which stress transfer is facilitated by hydrogen-bonding between the whiskers [43]. Additional reinforcement, depending on the nature of the polymer matrix, can be attributed to the interactions between the matrix and the whiskers. However, the whisker–whisker interactions can also cause whisker aggregation during the nanocomposite fabrication which, of course, limits the extent of mechanical reinforcement and as such also the potential mechanical switching contrast [41,44,45]. Thus, a critical step in maximising the difference in mechanical properties between the "on" and "off" state is to prepare evenly dispersed percolating nanocomposites.

Good dispersion can be achieved when interactions between whiskers are "switched off" during processing by competitive binding with a hydrogen-bond-forming solvent. Since water disperses most types of cellulose whiskers well the mixing of aqueous polymer solutions or emulsions with cellulose whisker suspensions and subsequent film casting has for a long time been the primary method to process polymer/whisker nanocomposites [46]. Further, several "solubilising schemes" have been explored to improve whisker dispersibility in organic media, including the use of surfactants [44,47], silylation [48], grafting of PEO [49] or maleated polypropylene [44], and acylation [50]. However, these surface modifications usually also reduce the interactions between the whiskers and thereby the macroscopic mechanical properties of the corresponding nanocomposites. Turbak, Dufresne, and some of us have shown that stable suspensions of tunicate whiskers with negatively charged sulfate groups, commonly produced by hydrolysis of the native cellulose with sulfuric acid [42,45,51], can also be produced in dimethylsulfoxide (DMSO) [52], *N*,*N*-dimethylformamide (DMF) [53,54], *N*-methylpyrrolidine (NMP) [54], formic acid [54], and *m*-cresol [54], for example by lyophilisation of aqueous whisker dispersions and re-dispersion of the resulting aerogel in the organic solvent [54]. Grey has produced similar cellulose whisker dispersions in polar organic solvents using whiskers obtained from cotton [55]. Cellulose whiskers without surface charges [56], prepared by hydrolysis with HCl, do not disperse as well in aprotic solvents (DMSO, DMF, NMP); however formic acid and *m*-cresol have been shown to also disperse non-charged whiskers properly [54]. We have demonstrated for a variety of host polymers (e.g. polystyrene, ethyleneoxide/epichlorohydrin copolymers, poly(vinylacetate)) that using a hydrogen-bond-forming solvent (e.g. dimethylformamide, DMF) allows to process polymer/whisker nanocomposites with properties that match the theoretical limit (vide infra) by solution casting: upon solvent evaporation the interactions between the whiskers are "switched on" and they assemble into a percolating network.

4.2. First generation dynamic nanocomposites based on EO–EPI

We reported a first generation of percolating cellulose whisker nanocomposites based on a 1:1 ethyleneoxide/epichlorohydrin copolymer (EO–EPI) matrix and systematically investigated such materials prepared with sulfonated tunicate whiskers [57]. EO–EPI was initially chosen as the polymer matrix on account of its low modulus ($E'_s = 3.7$ MPa) and its ability to uptake small amounts of water and other potential chemical regulators. Nanocomposite films were produced by solution-casting from DMF and also by a template approach [57]. The latter is based on the formation of a three-dimensional template scaffold of well-individualised whiskers, which is subsequently filled with a polymer of choice. The first step in this process is the formation of a nanofiber template through a sol/gel process. For cellulose whiskers this involves the formation of an aqueous whisker dispersion, which is converted into a gel through solvent-exchange with a water-miscible solvent, for example acetone, that "turns" the hydrogen bonding between the whiskers back on. This nanofiber template, which features a percolating network structure, is then filled with a matrix polymer by immersing the gel into a polymer solution, in a solvent that does not disperse the whiskers, and subsequent drying and shaping. Samples prepared by casting from DMF and the template approach displayed virtually identical mechanical properties [57]. In the rubbery regime, the tensile storage moduli (E'_c) of the dry EO–EPI-based materials at 25 °C increased by over two orders of magnitude from 3.7 MPa (neat EO–EPI) to ~800 MPa at a whisker content of ~19% (v/v). The magnitude of the reinforcement is related to the formation of a percolating nanofiber network in which stress transfer is facilitated by hydrogen-bonding between the cellulose whiskers. Using the experimentally determined values for the tensile storage modulus of the EO–EPI matrix, $E'_s = 3.7$ MPa, the whisker network, $E'_r = 4.0$ GPa (measured by DMTA of a solution-cast cellulose whisker film), the aspect ratio of the whiskers, $A = 84$ (determined from transmission electron microscopy images) Eqs. (1–2)

http://doc.rero.ch

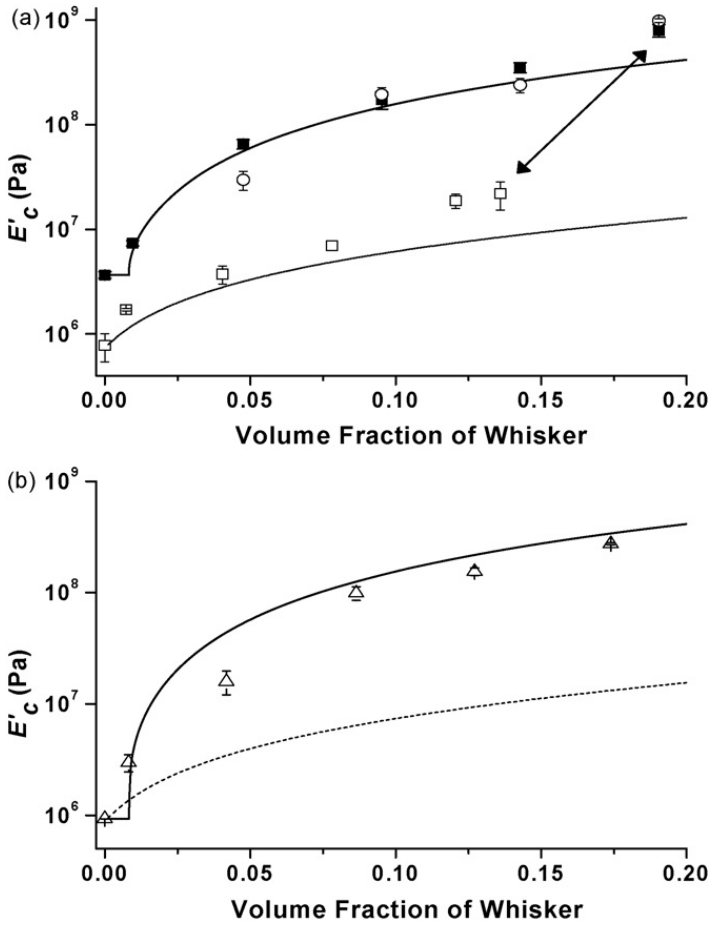

Fig. 3. (a) Tensile storage moduli E'_c of neat EO–EPI and EO–EPI/cellulose whisker nanocomposites in the dry state (■), swollen with deionised water (□), and re-dried after swelling with water (○); and (b) tensile storage moduli of neat EO–EPI and EO–EPI/cellulose whisker nanocomposites swollen with isopropyl alcohol (△). The lines show the values predicted by the percolation (solid) and the Halpin–Kardos (dashed) models. Reprinted from Ref. [58].

were employed to construct Fig. 3, which shows that the percolation model excellently matches the experimentally determined E'_c values of a series of EO–EPI nanocomposites comprising different volume fractions of cellulose whiskers isolated from tunicates [57]. It should be noted here that the value of $E'_r = 4$ GPa is lower than those observed by other groups, who have reported values as high as 15 GPa. Using our specific processing conditions [54] we consistently observe a value of between 4 and 9 GPa. The specific value of E'_r we employ corresponds to the modulus of the neat whisker sheet measured for the whisker batch from which the composite was made. Similar results were obtained for EO–EPI nanocomposites comprising cellulose whiskers isolated from cotton [57] and microcrystalline cellulose [45], albeit the aspect ratio of these fillers is much lower and their reinforcing effect is somewhat less pronounced.

After having demonstrated the ability to create nanocomposites in which the cellulose filler forms a percolating network, we next investigated the ability of these new materials to switch their mechanical behaviour in response to an external stimulus. Conceptually, the easiest way to turn "off" the whisker–whisker interactions is through the use of a chemical regulator known to disperse the whiskers (e.g. water). Gratifyingly, the tunicate cellulose nanocomposites based on an EO–EPI matrix discussed above (Fig. 3) exhibit a pronounced and reversible modulus reduction (e.g. from 800 to 20 MPa for a composite comprising 19% (v/v) cellulose whiskers at room temperature, i.e. 40-fold) upon exposure to water [58,59]. Fig. 3a shows that the E'_c values of water-swollen nanocomposite films more closely match the Halpin–Kardos than the percolation model [58]. (For this calculation the following values were used: tensile modulus of water plasticised EO–EPI, $E'_s = 0.8$ MPa, and the longitudinal Young's Modulus of the whisker, $E'_{lr} = 130$ GPa [34], the transverse Young's Modulus of the whisker, $E'_{tr} = 5$ GPa [34] and shear modulus of the whisker, $G_r = 1.77$ GPa [34], Poisson's ratios $\nu_r = 0.3$, $\nu_s = 0.5$ [34] and $A = 84$.) The water presumably disrupts the hydrogen bonding between the cellulose whiskers within the polymer matrix, and dissociates them from each other. At the same time, the water presumably also reduces the whisker–matrix interactions, although at this time we do not have experimental proof for this hypothesis. Removal of the water, by simply drying the films, was found to restore the original stiffness of the materials [58], consistent with the re-establishment of the whisker–whisker (and whisker–matrix) interactions.

To investigate the chemo-specificity of the switching mechanism, we investigated the effect that isopropanol (IPA) exerts on the mechanical behaviour of the EO–EPI/cellulose whisker nanocomposites. IPA was selected because it swells neat EO–EPI to a similar degree

http://doc.rero.ch

as water [58], but is incapable of dispersing cellulose whiskers [57]. Thus, while IPA should be able to swell the nanocomposites, there should be no dramatic reduction of the materials' modulus as the whisker interactions should remain intact. The nanocomposites indeed swelled upon immersion in IPA to a level similar to that of the composites in water; however except for the neat matrix polymer (which went from a dry value of 3.7 MPa to a IPA plasticised E'_s value of 0.93 MPa) E'_c barely changed in comparison to the dry state (Fig. 3b), and the experimental data still fit the percolation model derived from the resulting new value for E'_s [58]. This result is further evidence that the chemo-mechanical response is largely a result of disruption of the whisker–whisker interactions and not just simply plasticisation of the material.

4.3. Second generation dynamic nanocomposites based on PVAc

With the motivation of possibility of using such materials as mechanically adaptable, implantable biomedical devices, and with the goal to further enhance the contrast between the soft and hard states of these nanocomposites, we set out to explore a second generation of nanocomposites that combines the bio-inspired switching mechanism with a chemically influenced thermal transition. In this scenario, the material should be stiff when dry and at room temperature but exhibit a significant modulus change upon immersion into a biologically relevant fluid (e.g. artificial cerebrospinal fluid, ACSF) at 37 °C. We discovered that nanocomposites based on poly(vinyl acetate) (PVAc, T_g ca. 42–56 °C, depending on annealing conditions and method of measurement [60]) and cellulose whiskers display such a "dual" responsive behaviour [57,58] and here give a more detailed account of our in-depth study of this system. All data reported herein were reproduced using new batches of whiskers and nanocomposites. The experimental procedures followed those previously published [58] except that the new films, after casting from DMF solutions, were dried for 1 week as opposed to 2 days in a vacuum oven at 65 °C. The agreement of the data is within experimental error.

Fig. 4a displays the temperature-dependent tensile storage moduli (DMTA traces) for these PVAc/whisker nanocomposites in the dry state. The neat PVAc matrix exhibits a DMTA trace that is typical of an amorphous polymer, with an E'_s of ~1.8 GPa in the glassy state (23 °C). Upon increasing the temperature beyond 30 °C, E'_s drops drastically to reach ~1 MPa at 70 °C, owing to the onset of the T_g of the polymer. Below T_g, the PVAc/cellulose whisker nanocomposites showed a only a modest increase of the tensile storage modulus upon introduction of the rigid filler; E'_c increased from 1.8 GPa for the neat polymer to 5.4 GPa for a nanocomposite comprising 16.5% (v/v) cellulose whiskers. This is typical of composites reinforced with rigid fillers and is consistent with other studies on cellulose whisker nanocomposites [31,39]. Tunicate cellulose whiskers have been reported to have a modulus greater than 130 GPa [43], which is roughly two orders of magnitude higher than the matrix modulus, and if incorporated into a matrix polymer in substantial amounts should augment the load bearing and deformation resistance behaviour of the composites. As is evident from Fig. 4a, the modulus reduction around T_g was much less pronounced for the nanocomposites than the neat polymer and the modulus in the rubbery plateau was significantly higher. To understand the factors at play behind this stabilisation, the DMTA loss tangent (tanδ) of the materials were analysed (Fig. 4b).

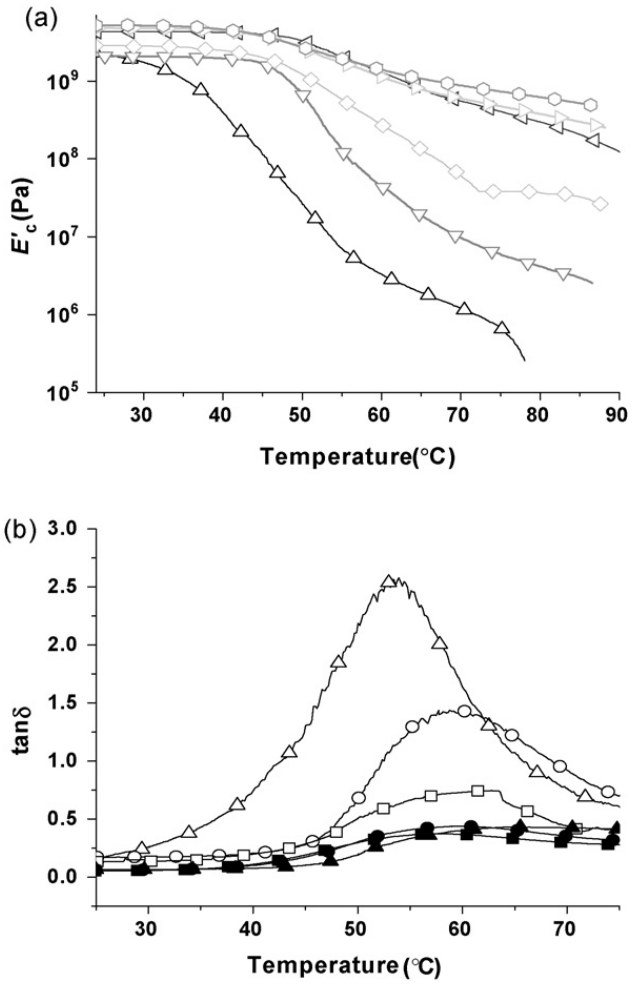

Fig. 4. (a) Tensile storage moduli E'_c of dry films of neat PVAc and PVAc/tunicate whisker (TW) nanocomposites as a function of temperature and composition: 0% (v/v) TW (△), 0.8% (v/v) TW (○), 4% (v/v) TW (□), 8.1% (v/v) TW (▲), 12.2% (v/v) TW (●), 16.5% (v/v) TW (■). Data were acquired by dynamic mechanical thermoanalysis (DMTA). (b) Loss tangent vs. temperature plots of DMTA sweeps shown in (a).

Tanδ is the ratio of loss modulus to storage modulus of the material, and is indicative of its damping behaviour. A peak in the tanδ vs. temperature trace reflects a loss of energy due to the relaxation processes in polymeric materials, and in the case of the present materials is related to the glass transition. The peak temperature (T_α) corresponds to the transition temperature and the intensity (I_α) is related to the magnitude of the relaxation [62]; Data extracted from Fig. 4b for neat PVAc and the PVAc/tunicate whisker nanocomposites are compiled in Table 1. T_α is relatively constant and is observed around 60 °C (±4 °C) regardless of whisker content (although one may interpret that the data show a slight increase of T_α). This indicates that the T_g of the nanocomposites remained largely unaffected by the incorporation of cellulose whiskers. However, I_α was dras-

http://doc.rero.ch

Table 1
Tanδ peak temperature and predicted and observed intensity, I_α, of neat PVAc and PVAc/tunicate whisker nanocomposites as a function of composition.

Sample	T_α (°C)	Predicted I_α	Observed I_α
Neat PVAc	56	2.50	2.50
0.8% (v/v) TW PVAC	58.2	2.48	1.39
4.0% (v/v) TW PVAc	62.9	2.40	0.67
8.1% (v/v) TW PVAc	64.6	2.30	0.43
12.2% (v/v) TW PVAc	62.3	2.19	0.39
16.5% (v/v) TW PVAc	60.5	2.09	0.39

tically reduced. In general, filler-reinforced polymers can be expected to show a slight reduction in I_α, with increasing filler concentration, which can be attributed to a reduced fraction of the matrix material and hence number of mobile units. Neilsen suggested that I_α of the composite can be predicted by $I_{\alpha c} = I_{\alpha s}(1-\upsilon_r)$, where $I_{\alpha c}$ and $I_{\alpha s}$ refer to tanδ peak intensities of the nanocomposite and neat polymer respectively and υ_r is the filler volume fraction [61]. However, as can be seen in Table 1, the observed reduction in I_α with an increase in filler concentration is much higher than is predicted based on υ_r. It should be noted here that the T_g value of the neat PVAc we measured using DMTA was ca. 56 °C.

Dufresne et al. reported a similar behaviour in tunicate whisker reinforced nanocomposites and attributed the significant reduction of the intensity of I_α to polymer–whisker interactions [62]. Considering the numerous hydrogen bonding opportunities between the PVAc matrix and the hydrophilic cellulose whiskers, it is indeed likely that the matrix–whisker interactions contribute to the pronounced reduction in magnitude of chain relaxation and hence I_α, The values of the dry moduli reported here are about 10–20% higher than those of nominally identical materials we reported before [60]. We relate this difference primarily to the intrinsic experimental error associated with the difficulty to accurately determine the thickness of soft thin films [60]. We also changed the drying procedure vis a vis our initial protocol; the different thermal history also appears to influence the thermomechanical properties of the nanocomposites, as we observe a 12–16 °C increase in the tanδ peaks compared to our initial data. The longer drying times of the more recent solution-cast films rigorously eliminate trace amounts of solvent that otherwise results in plasticisation and lower T_g, although we also cannot rule out annealing effects [60].

Fig. 4a shows that the relative magnitude of the mechanical reinforcement of the PVAc/cellulose whisker nanocomposites is much more significant above T_g than below. Fig. 5 shows a plot of the tensile storage moduli E'_c of dry films at 70–80 °C (i.e. in the rubbery regime, ~12–16° above T_g). The experimental data (solid squares) closely follow the prediction of the percolation model, confirming again the formation of a cellulose whisker network within the PVAc matrix.

Fig. 6 shows the swelling behaviour of neat PVAc and PVAc/cellulose whisker nanocomposites that have been immersed in deionised water at room temperature (23 °C, 1 week equilibrium), as well as samples that have been immersed in either deionised water or ACSF at simulated

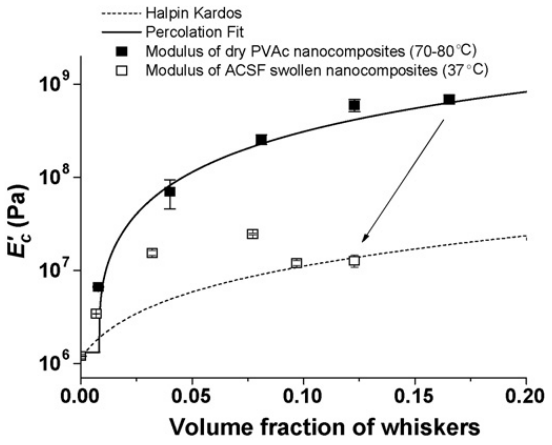

Fig. 5. Tensile storage moduli E'_c of neat PVAc and PVAc/cellulose whisker nanocomposites in the dry state (70–80 °C) (■), swollen with ACSF (37 °C for 1 week) (□). The lines show the values predicted by the percolation (solid) and the Halpin–Kardos (dashed) models. Data of swollen samples are at a lower volume fraction compared to their dry state after considering water uptake.

body temperature (37 °C, 1 week equilibrium). The swelling ratio, or relative water uptake, increased with the whisker content for both solvents and at both 23 °C as well as 37 °C. This effect can be attributed to the increased hydrophilicity of the nanocomposite on account of the presence of cellulose whiskers. Evaluation at room temperature revealed a steady increase in swelling ratio with increasing whisker concentration. At 37 °C this effect was much more pronounced. The higher degree of swelling of PVAc/whisker nanocomposites at 37 °C as compared to 23 °C can be attributed to the increase of the free volume above T_g. Previous swelling studies at room temperature and 98% RH had shown that the aqueous swelling ratio of PVAc initially increases upon addition of cellulose whiskers, but levels off at a whisker content of ~5–10 wt.% [63]. Swelling conditions can significantly influence the swelling ratio and hence, a direct comparison between this study and the pre-

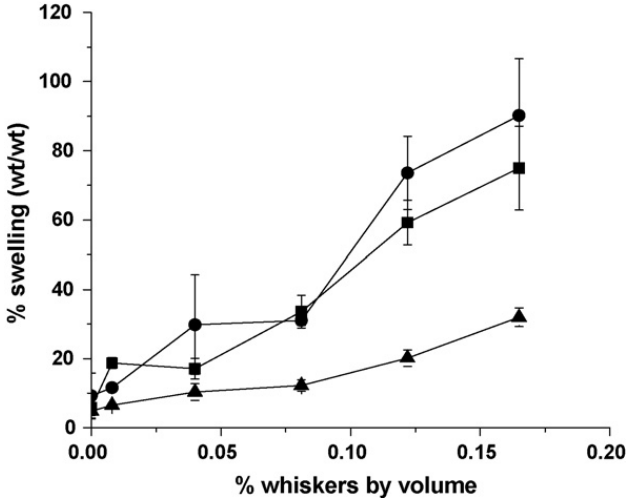

Fig. 6. Swelling of PVAc/whisker nanocomposites. Water uptake as a function of whisker volume fraction and temperature upon immersion (to equilibration) in deionised water or ACSF. Data points represent averages (N = 3–5) ± standard deviation measurements. Deionised water (23 °C) (▲), deionised water (37 °C) (■) and ACSF (37 °C) (●).

http://doc.rero.ch

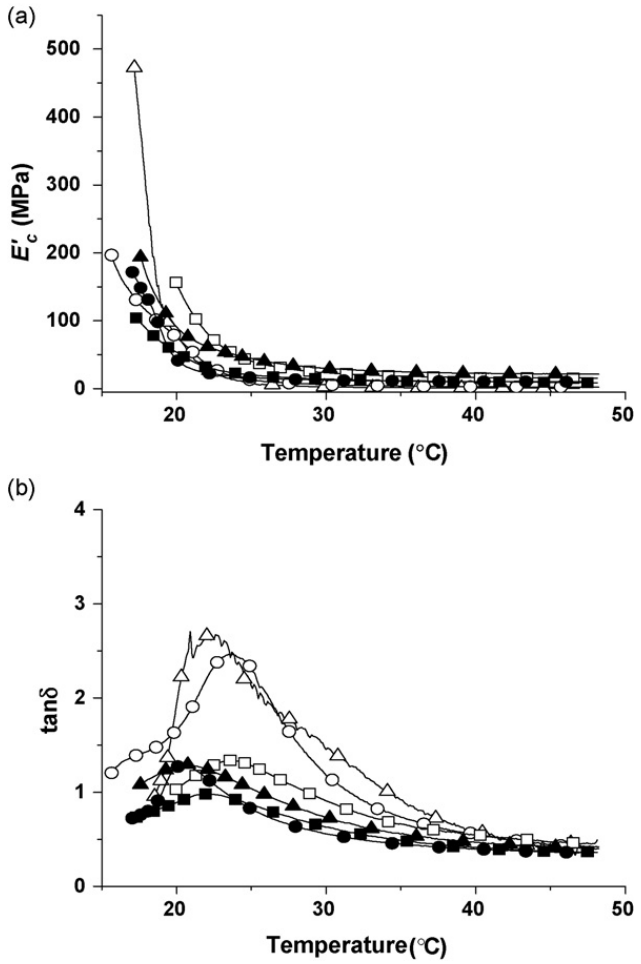

Fig. 7. (a) Tensile storage moduli E'_c of ACSF swollen (for 1 week at 37 °C) films of neat PVAc and PVAc/tunicate whisker (TW) nanocomposites as a function of temperature and composition: 0% (v/v) TW (△), 0.8% (v/v) TW (○), 4% (v/v) TW (□), 8.1% (v/v) TW (▲), 12.2% (v/v) TW (●) and 16.5% (v/v) TW (■). Data were acquired by dynamic mechanical thermoanalysis (DMTA). (b) Loss tangent vs. temperature plots of DMTA sweeps shown in (a).

vious one may be misleading due to the different swelling conditions and range of whisker concentration studied.

The tensile storage moduli E'_c of neat PVAc and PVAc/cellulose whisker nanocomposite samples that had been immersed in ACSF at 37 °C for 1 week (i.e. to equilibrium) were determined using a DMTA set-up with submersion clamp, which allowed to keep the samples immersed in ACSF during the tests. DMTA traces (Fig. 7a) and the corresponding tanδ plots (Fig. 7b) show that the T_g has dropped to 21 ± 2 °C for the swollen samples owing to plasticisation of matrix polymer. As a consequence, the plasticised PVAc and nanocomposites display very low tensile storage moduli (ranging from 1 to 12 MPa) at 37 °C, i.e. in the rubbery plateau. This is over 3 orders of magnitude less than their dry moduli at an identical temperature. Interestingly, the nanocomposites with higher whisker content had a lower wet modulus compared to the nanocomposites with lower whisker content. This can be attributed to the higher swelling ratio of high whisker content nanocomposites since normalising the modulus reduction with the corresponding swelling ratio revealed a similar extent of reduction in modulus in all the nanocomposites.

Under dry conditions at temperatures well above T_g, nanocomposites displayed orders of magnitude higher modulus than the neat matrix, which was attributed to the strong interconnected whisker network. Upon swelling with water the nanocomposites became as soft as neat matrix polymer which is not possible with an intact network of whiskers. This suggests that, in addition to plasticisation of matrix, water also disrupts the whisker network breaking the hydrogen bonds between them. While the experimental storage modulus of the dry samples closely followed the percolation model, the modulus of swollen samples at 37 °C (12–16 °C) above the T_g of the polymer) more closely fits the Halpin Kardos model (using E'_s value of the swollen PVAc matrix of 1.2 MPa) at the higher concentration of whiskers, where there is substantial water diffusion into the film to disrupt the whisker network (Fig. 5). This supports the hypothesis that in the swollen state the whiskers are no longer connected extensively by hydrogen bonds, either through whisker–whisker interactions nor whisker–matrix interactions.

Addition of whiskers to PVAc increased the moduli of the dry materials to between 4 and 5 GPa below the T_g. On exposure to thermal and chemical stimuli (water or ACSF) the nanocomposites became as soft as neat matrix demonstrating stimuli responsive dynamic modulus behaviour of PVAc nanocomposites. The temperature range (23 °C to 37 °C) within which drastic modulus change can be achieved in this system is what makes it particularly attractive as a dynamic material for possible biomedical applications. A room temperature modulus around 4–5 GPa would render sufficient rigidity for penetrating implantation into soft tissue, and a soft state modulus of 1–12 MPa being closer to the modulus of softer tissues (i.e. brain) could theoretically minimise biocompatibility issues due to mechanical mismatch.

For use as biomaterials, the rate at which the material changes from stiff to soft under physiological conditions may prove to be critical. Therefore, the nanocomposites were immersed into ACSF within the confines of the DMTA and the temperature was ramped from 23 °C to 37 °C over a period of 13 min at which point it was held isothermally at 37 °C for an hour. The presence of ACSF in conjunction with the increase in temperature resulted in a drastic decrease in modulus from ~4400 MPa to 60 MPa within the 13 min temperature ramp period (Fig. 8). When the material was held isothermally at 37 °C for 30 min, the modulus further reduced closer to that of neat PVAc. On the other hand, the neat PVAc modulus drops to 200 MPa by the time the first data point is taken (minutes from clamping time) and is further reduced over time to ca. 1.05 MPa.

Within the scope of this experiment, which simulates the incorporation into tissue, neat PVAc undergoes a significant (orders of magnitude) change in modulus by just thermal stimulus alone, because it is heated to above T_g. However some practical difficulties are involved if it is to be used alone as a thin film for implantation into the body. The modulus in dry state might still be low for certain applications. More importantly, rapid heat transfer through the thin films could result in premature softening during inser-

http://doc.rero.ch

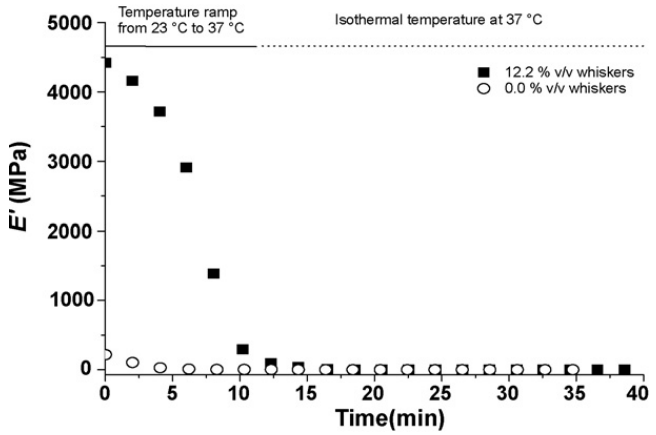

Fig. 8. Time-dependent modulus decrease of dry neat PVAc (○) and a 12.2% (v/v) PVAc/whisker nanocomposite (■) upon immersion into ACSF and increasing the temperature from 23 °C to 37 °C. Lines represent time required for temperature to increase from 23 °C to 37 °C and isothermal control at 37 °C.

tion. Incorporation of whiskers not only helps to increase the modulus of PVAc from 1.8 to 5.4 GPa for 16.5% (v/v) whiskers, but unlike the neat polymer, the nanocomposites also retain the modulus until above body temperature – retaining its rigidity for insertion into physiological tissue. This system now depends on two stimuli and two different effects, plasticisation of PVAc matrix and disruption of whisker network to manifest a dynamic change in modulus. Exposure to chemical stimuli such as water or physiological fluids plasticises the matrix and lowers the T_g of the matrix polymer softening the matrix. The modulus of the composite thus depends primarily on the hydrogen bonded whisker network which in turn is disrupted by water or physiological fluids to yield a very soft material. If temperature is the only stimulus required, the material can become soft within the time scale of insertion as it undergoes a temperature change. However, the dependence on a second mechanism, water or any physiological fluid, to break the percolating network of hydrogen bonded whiskers makes the system diffusion controlled, and the transition from stiff to soft can more readily be tailored to a desired time scale.

5. Conclusions

Biological systems continue to inspire materials scientists and engineers alike [64,65]. In this review we have outlined how the dermis of the sea cucumber inspired the design of a new class of mechanically responsive nanocomposites. Of course one of the key aspects in any biomimetic material is an understanding of how nature achieves the specific materials properties required by the plant or animal. In this case it was pioneering work by a range of scientist to start to piece together the mechanism by which the sea cucumber can change the stiffness of its inner dermis. Thus inspired by the sea cucumber and building on the elegant work of these scientists it has been possible to retro-engineer a synthetic nanocomposite that mimics the architecture and also the properties of the sea cucumber dermis. The first few generations of these mechanically adaptable nanocomposites are chemo-responsive, using water to mediate the interaction between the whiskers. One of the advantages of a synthetic system is the ability to introduce other effects into the mimetic biological design. This was achieved in the 2nd generation PVAc nanocomposites where, in conjunction to nanocomposite switching mechanism, a water induced thermal transition was also utilised to further enhance the mechanical contrast allowing changes from ca. 5 GPa in the stiff state to ca. 5 MPa in the soft state, compared to the 50 MPa to 5 MPa observed for the sea cucumber. Of course, there is still a long way to go to achieve some of the properties of the natural model. For example, the switching rate in the sea cumber dermis in less than a second, while the current generations of synthetic mimics are diffusion controlled and so switching is much slower. Depending on the nature of the application this may or may not be beneficial. However, one advantage that the synthetic systems do have is that by using the same basic whisker disengagement strategy it may be possible to use other stimuli (such as electrical or light) to induce the mechanical response, which we are currently pursuing.

Acknowledgments

We thank F. Carpenter for the photography of the sea cucumber and acknowledge generous financial support from DuPont (Young Professor Award to C.W.), the L. Stokes Cleveland VAMC Advanced Platform Technology Center, an Ohio Innovation Incentive Fellowship (to K.S.), from the Department of Veterans Affairs Career Development Program (to J.C., Grant# F4827H), and the National Institute of Health (Grant# R21NS053798-0).

References

[1] Shahinpoor M, Schneider H-J, editors. Intelligent Materials. Cambridge UK: RSC Publishing; 2004.
[2] (a) Lendlein A, Kelch S. Shape-memory polymers. Angew Chem Int Ed 2002;41:2034–57;
(b) Liu C, Qin H, Mather PT. Review of progress in shape-memory polymers. J Mater Chem 2007;17:1543–58.
[3] Lendlein A, Langer R, Biodegradable. elastic shape-memory polymers for potential biomedical applications. Science 2002;296:1673–6.
[4] Lendlein A, Jiang H, Juenger O, Langer R. Light-induced shape-memory polymers. Nature 2005;434:879–82.
[5] Kainuma R, Imano Y, Ito W, Sutou Y, Morito H, Okamoto S, et al. Magnetic-field-induced shape recovery by reverse phase transformation. Nature 2006;439:957–60.
[6] de las Heras Alarcón C, Pennadam S, Alexander C. Stimuli responsive polymers for biomedical applications. Chem Soc Rev 2005;34:276–85.
[7] Jaber JA, Schlenoff JB. Mechanical properties of reversibly cross-linked ultrathin polyelectrolyte complexes. J Am Chem Soc 2006;128:2940–7.
[8] Loveless DM, Jeon SL, Craig SL. Chemoresponsive viscosity switching of a metallo-supramolecular polymer network near the percolation threshold. J Mater Chem 2007;17:56–61.
[9] See for example Suzuki T, Shinkai S, Sada K. Supramolecular crosslinked linear poly(trimethylene iminium trifluorosulfonimide) polymer gels sensitive to light and thermal stimuli. Adv Mater 2006;18:1043–6.
[10] Warner M, Terentjev EM. Liquid Crystal Elastomers. Oxford: Clarendon Press; 2003.
[11] Minagawa K, Koyama K. Electro- and magneto-rheological materials: stimuli-induced rheological functions. Curr Org Chem 2005;16:1643–63.
[12] (a) See for example Pelrine R, Kornbluh R, Pei QB, Joseph J. High-speed electrically actuated elastomers with strain greater than 100%. Science 2000;287:836–9;
(b) Ebron VH, Yang ZW, Seyer DJ, Kozlov ME, Oh JY, Xie H, et al. Fuel-powered artificial muscles. Science 2006;311:1580–3.

http://doc.rero.ch

[13] Yoshida R. Design of functional polymer gels and their application to biomimetic materials. Curr Org Chem 2005;16:1617–41.
[14] (a) Needham D, Dewhirst MW. The development and testing of a new temperature-sensitive drug delivery system for the treatment of solid tumors. Adv Drug Deliv Rev 2001;53:285–305;
(b) Peppas NA, Hilt JZ, Khademhosseini A, Langer R. Hydrogels in biology and medicine: from molecular principles to bionanotechnology. Adv Mater 2006;18:1345–60.
[15] (a) Shimuzu T, Yamato M, Kikuchi A, Okano T. Two-dimensional manipulation of cardiac myocyte sheets utilizing temperature-responsive culture dishes augments the pulsatile amplitude. Tissue Eng 2001;7:141–51;
(a) Kwon OH, Kikuchi A, Yamato M, Sakurai Y, Okano T. Rapid cell sheet detachment from poly(*N*-isopropylacrylamide)-grafted porous cell culture membranes. J Biomed Mater Res 2000;50:82–9.
[16] Heinzeller T, Nebelsick J, editors. Echinoderms. London: Taylor & Francis Group; 2004.
[17] Motokawa T. The stiffness change of the holothurian dermis caused by chemical and electrical stimulation. Compl Biochem Physiol 1996;5:61–102.
[18] Wilkie IC. Mutable collagenous tissues: Extracellular matrix as mechano-effector. Echinoderm Stud 1996;5:61–102.
[19] Trotter JA, Thurmond FA. Morphology and biomechanics of the microfibrillar network of sea cucumber dermis. J Exp Biol 1996;199:1817–28.
[20] Wilkie IC. Is muscle involved in the mechanical adaptability of echinoderm mutable collagenous tissue? J Exp Biol 2002;205:159–65.
[21] Trotter JA, Koob TJ. Evidence that calcium-dependent cellular processes are involved in the stiffening response of holothurian dermis and that dermal cells contain an organic stiffening factor. J Exp Biol 1995;198:1951–61.
[22] Szulgit GK, Shadwick RE. Dynamic mechanical characterization of a mutable collageneous tissue: response of sea cucumber dermis to cell lysis and dermal extracts. J Exp Biol 2000;203:1539–50.
[23] Trotter JA, Lyons-Levy G, Luna D, Koob TJ, Keene DR, Atkinson MAL, et al. A glycoprotein from sea cucumber dermis that aggregates collagen fibrils. Matrix Biol 1996;15:99–110.
[24] Trotter JA, Lyons-Levy G, Chino K, Koob TJ, Keene DR, Atkinson MAL. Collagen fibril aggregation inhibitor from sea cucumber dermis. Matrix Biol 1999;18:569–78.
[25] Koob TJ, Koob-Edmunds MM, Trotter JA. Cell-derived stiffening and plasticizing factors in sea cucumber (*Cucumaria frondosa*) dermis. J Exp Biol 1999;202:2291–301.
[26] Tipper JP, Lyons-Levy G, Atkinson MAL, Trotter JA. Purification, characterization and cloning of tensilin, the collagen-fibril binding and tissue-stiffening factor from *Cucumaria frondosa* dermis. Matrix Biol 2003;21:625–35.
[27] Trotter JA, Tipper J, Lyons-Levy G, Chino K, Heuer AH, Liu Z, et al. Towards a fibrous composite with dynamically controlled stiffness: lessons from echinoderms. Biochem Soc Trans 2000;28:357–62.
[28] Dalmas F, Cavaillé JY, Gauthier C, Chazeau L, Dendievel R. Viscoelastic behavior and electrical properties of flexible nanofibers filled polymer nanocomposites. Influence of processing conditions. Comp Sci Technol 2007;67:829–39.
[29] Takayanagi M, Uemura S, Minami S. Application of equivalent model method to dynamic rheo-optical properties of a crystalline polymer. J Polym Sci C 1964;5:113–22.
[30] Ouali N, Cavaillé JY, Pérez J. Elastic, viscoelastic and plastic behavior of multiphase polymer blends. Plast Rubber Comp Process Appl 1991;16:55–60.
[31] Favier V, Chanzy H, Cavaillé JY. Polymer nanocomposites reinforced by cellulose whiskers. Macromolecules 1995;28:6365–7.
[32] Favier V, Dendievel R, Canova G, Cavaille JY, Gilormini P. Simulation and modeling of three-dimensional percolating structures: case of a latex matrix reinforced by a network of cellulose fibers. Acta Mater 1997;45:1557–65.
[33] Halpin JC, Kardos JL. Moduli of crystalline polymers employing composite theory. J Appl Phys 1972;43:2235–41.
[34] Hajji P, Cavaillé J-Y, Favier V, Gauthier C, Vigier G. Tensile behavior of nanocomposites from latex and cellulose whiskers. Polym Composites 1996;17:612–9.
[35] Ramirez MG, Cavaillé J-Y, Dufresne A, Tekly P. Cellulose-polyamide 66 blends. Part II: Mechanical behavior. J Polym Sci Part B Polym Phys 1995;33:2109–24.
[36] Favier V, Canova GR, Shrivastava SC, Cavaille JY. Mechanical percolation in cellulose whisker nanocomposites. Polym Eng Sci 1997;37:1732–9.
[37] Grunlan JC, Liu L, Kim YS. Reversible control of single-walled carbon nanotube microstructure using poly(acrylic acid). Nano Lett 2006;6:911–5.
[38] Favier V, Canova GR, Cavaille JY, Chanzy H, Dufreshne A, Gauthier C. Nanocomposite materials from latex and cellulose whiskers. Polym Adv Tech 1995;6:351–5.
[39] Ljungberg N, Cavaillé J-Y, Heux L. Nanocomposites of isotactic polypropylene reinforced with rod-like cellulose whiskers. Polymer 2006;47:6285–92.
[40] Helbert W, Cavaillé J-Y, Dufresne A. Thermoplastic nanocomposites filled with wheat straw cellulose whiskers. Part I: Processing and mechanical behavior. Polym Comp 1996;18:604–11.
[41] Schroers M, Kokil A, Weder C. Solid polymer electrolytes based on nanocomposites of ethylene oxide-epichlorohydrin copolymers and cellulose whiskers. J Appl Polym Sci 2004;93:2883–8.
[42] de Souza Lima MM, Borsali R. Rodlike cellulose microcrystals: structure, properties, and applications. Macromol Rapid Commun 2004;25:771–87.
[43] Sturcova A, Davies JR, Eichhorn SJ. Elastic modulus and stress-transfer properties of tunicate cellulose whiskers. Biomacromolecules 2005;6:1055–61.
[44] Ljungberg N, Bonini C, Bortolussi F, Boisson C, Heux L, Cavaillé J-Y. New nanocomposite materials reinforced with cellulose whiskers in atactic polypropylene: effect of surface and dispersion characteristics. Biomacromolecules 2005;6:2732–9.
[45] Capadona JR, Shanmuganathan K, Trittschuh S, Seidel S, Rowan SJ, Weder C. Polymer nanocomposites with microcrystalline cellulose. Biomacromolecules 2009;10:712–6.
[46] Samir MASA, Alloin F, Dufresne A. Review of recent research into cellulosic whiskers, their properties and their application in nanocomposite field. Biomacromolecules 2005;6:612–26.
[47] Bonini C, Heux L, Cavaillé J-Y, Lindner P, Dewhurst C, Terech P. Rodlike cellulose whiskers coated with surfactant: a small-angle neutron scattering characterization. Langmuir 2002;18:3311–4.
[48] Gousse C, Chanzy H, Excoffier G, Soubeyrand L, Fleury E. Stable suspensions of partially silylated cellulose whiskers dispersed in organic solvents. Polymer 2002;42:2645–51.
[49] Araki JM, Wada M, Kuga S. Steric stabilization of a cellulose microcrystal suspension by poly(ethylene glycol) grafting. Langmuir 2001;17:21–7.
[50] Yuan H, Nishiyama Y, Wada M, Kuga S. Surface acylation of cellulose whiskers by drying aqueous emulsion. Biomacromolecules 2006;7:696–700.
[51] Marchessault RH, Morehead FF, Walter NM. Liquid crystal systems from fibrillar polysaccharides. Nature 1959;184:632–3.
[52] Turbak A, Snyder F, Sandberg K. Suspensions containing microfibrillataed cellulose, US Patent 4,378,381; 1983.
[53] (a) Samir MASA, Alloin F, Sanchez JY, El Kissi N, Dufresne A. Preparation of cellulose whiskers reinforced nanocomposites from an organic medium suspension. Macromolecules 2004;37:1386–93;
(b) Marcovich NE, Auad ML, Bellesi NE, Nutt SR, Aranguren MI. Cellulose micro/nanocrystals reinforced polyurethane. J Mater Res 2006;21:870–81.
[54] van den Berg O, Capadona JR, Weder C. Preparation of homogeneous dispersions of tunicate cellulose whiskers in organic solvents. Biomacromolecules 2007;8:1353–7.
[55] Viet D, Beck-Candanedo S, Gray DG. Dispersion of cellulose nanocrystals in polar organic solvents. Cellulose 2007;14:109–13.
[56] (a) Araki J, Wada M, Kuga S, Okano T. Flow properties of microcrystalline cellulose suspension prepared by acid treatment of native cellulose. Coll Surf A 1998;142:75–82;
(b) Araki J, Wada M, Kuga S, Okano T. Birefringent glassy phase of a cellulose microcrystal suspension. Langmuir 2000;16:2413–5.
[57] Capadona JR, van den Berg O, Capadona L, Schroeter M, Tyler DJ, Rowan SJ, et al. A versatile approach for the processing of polymer nanocomposites with self-assembled nanofiber templates. Nat Nanotechnol 2007;2:765–9.
[58] Capadona JR, Shanmuganathan K, Tyler DJ, Rowan SJ, Weder C. Stimuli-responsive polymer nanocomposites inspired by the sea *Cucumber Dermis*. Science 2008;319:1370–4.
[59] (a) Bellamkonda RV. Marine inspiration. Nat Mater 2008;7:347–8;
(b) Craig SL. Cool as a cucumber. Angew Chem Int Ed 2008;47:8776–7.
[60] Bair HE. Measurement of glass transition by DSC. In: Seyler RJ, editor. Assignment of the Glass Transition. Baltimore MD: ASTM International; 1994. p. 50–74.
[61] Nielsen LE. Dynamic mechanical properties of filled polymers. Appl Polym Symp 1969;12:249–65.

http://doc.rero.ch

[62] Dufresne A. Interfacial phenomena in nanocomposites based on polysaccharide nanocrystals. Comp Interfaces 2003;10:369–87.
[63] Rodriguez NG, Thielemans W, Dufresne A. Sisal cellulose whiskers reinforced polyvinyl acetate nanocomposites. Cellulose 2006;13:261–70.
[64] For a special issue on Biological and Biomimetic Materials see Aizenberg J, Fratzl P, editors. Adv Mater 2009;21:379–494.
[65] Vincent JFV. Biomimetic materials. J Mater Res 2008;23:3140–7.

http://doc.rero.ch